Thermal-strain-induced splitting of heavy- and light-hole exciton energies in CuI thin films grown by vacuum evaporation

D. Kim, M. Nakayama, O. Kojima, I. Tanaka, H. Ichida, T. Nakanishi, and H. Nishimura

Department of Applied Physics, Faculty of Engineering, Osaka City University, Sugimoto 3-3-138, Sumiyoshi-ku, Osaka 558-8585, Japan

(Received 3 June 1999)

We have investigated thermal strain effects on excitons in CuI thin films with a thickness of 10–3000 nm grown by vacuum evaporation onto (0001) Al_2O_3, fused silica (quartz), and (001) NaCl substrates. The x-ray-diffraction patterns indicate that the crystalline thin film grown on every substrate is preferentially oriented along the $\langle 111 \rangle$ crystal axis. All the absorption spectra for the films with a thickness of 10–100 nm clearly show a doublet structure of the heavy-hole and light-hole excitons which are degenerate under a strain-free condition: The heavy-hole exciton has the higher energy for the Al_2O_3 and quartz substrates, while it has the lower energy for the NaCl one. The splitting energy increases as temperature decreases. This indicates that the in-plane strain, which results from the difference of the thermal expansion coefficients of CuI and the substrate, induces the splitting. The critical layer thickness for the thermal strain relaxation in the Al_2O_3 substrate is estimated to be 400 nm from the observed exciton energies as a function of the layer thickness. The shifts of the exciton energies due to the thermal strain effects are successfully analyzed on the basis of a $k \cdot p$ perturbation theory. [S0163-1829(99)04543-9]

I. INTRODUCTION

Optical properties of excitons in semiconductors with the reduced dimensionality such as quantum wells, wires, and dots have attracted much attention because the transition energy of the exciton can be controlled by the quantum size effect. In addition, there is another important effect in thin-film structures resulting from the existence of a substrate: strain effects. There are two kinds of strains in thin films: lattice-mismatch and thermal strains. The lattice-mismatch strain arises during the growth process if the lattice constants of substrates and layer do not coincide at the growth temperature. The thermal strain is caused by the cooling process from the growth temperature to the temperature at which optical measurements are performed owing to the difference of thermal expansion coefficients between the substrates and films. Thus, there are possibilities that we can control the exciton energies by choosing substrate materials and the growth temperature.

Cuprous halides have been a model material for the investigation of excitonic properties because excitons in these crystals have large binding energies: 190 meV for CuCl, 108 meV for CuBr, and 62 meV for CuI.[1] The symmetry of the cuprous halides belongs to T_d, and the optical transition is of a direct allowed type at the Γ point. The excitons consisting of holes of $j_h = 3/2$ and 1/2 are called the $Z_{1,2}$ and Z_3 excitons, respectively: The $Z_{1,2}$ exciton corresponds to the degenerate heavy-hole (HH) and light-hole (LH) excitons at the Γ point, and the Z_3 exciton to the split-off-hole exciton. Blacha *et al.* reported the uniaxial strain effect on the exciton transition in CuCl, CuBr, and CuI films with the thickness of ~ 2000 Å and determined the deformation potentials for the hydrostatic and shear stress.[2] For the thermal strain effect, Ageev *et al.* studied optical absorption spectra of CuI films and discussed the thermal-strain-induced splitting of the $Z_{1,2}$ exciton lines.[3] They, however, have not reported the details of the spectral features. Although several groups have investigated excitonic properties of thin films of the other cuprous halides such as CuCl and CuBr,[4,5] the thermal strain effect has not been observed in these materials so far. Since the magnitude of the thermal strain essentially depends on the measurement temperature, it is quite important for the investigation of the thermal strain effect to measure the temperature dependence of optical spectra of excitons. However, there has been no report on the temperature dependence. The film-thickness dependence of the thermal strain has also remained as an unsolved problem. Moreover, it is noted that the thermal strain effect is one of essential factors to control excitonic properties.

In the present work, we have investigated CuI thin films with the thickness of 10–3000 nm grown by vacuum evaporation onto (0001) Al_2O_3, fused silica (quartz), and (001) NaCl substrates. The thin films are crystalline and preferentially oriented along the $\langle 111 \rangle$ crystal axis. The absorption spectra show clear doublet structures around $Z_{1,2}$ exciton energies. The doublet structures are due to the splitting of the heavy-hole- and light-hole-exciton energies, which is caused by in-plane biaxial strains. Since the splitting becomes smaller with the increase of the temperature, the origin of the biaxial strains is considered to be the thermal strain. From the layer-thickness dependence of the exciton energies, it is found that the thermal strain in CuI films grown on Al_2O_3 begins to relax at 500 nm and fully vanishes at 3000 nm. The thermal strain effects on the exciton energies are quantitatively analyzed on the basis of a $k \cdot p$ perturbation theory.

II. EXPERIMENTAL PROCEDURE

Thin films of CuI with the layer thickness of 10–3000 nm were grown on (0001) Al_2O_3 (sapphire), quartz, and (001) NaCl substrates at $\sim 170\,^{\circ}C$ using a vacuum deposition

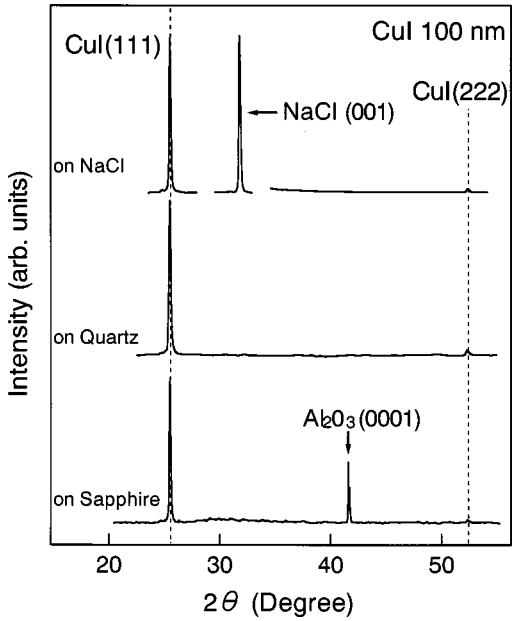

FIG. 1. $\theta-2\theta$ x-ray diffraction patterns measured at room temperature for the CuI thin films with the thickness of 100 nm grown on the sapphire, quartz, and NaCl substrates.

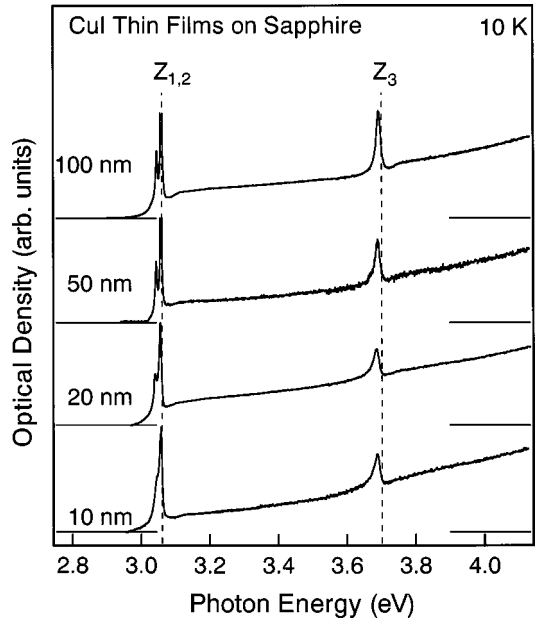

FIG. 2. Absorption spectra at 10 K for the CuI thin films with the thickness of 10, 20, 50, and 100 nm grown on the sapphire substrate. The broken lines depicted at 3.06 and 3.70 eV represent the $Z_{1,2}$ and Z_3 exciton energies in CuI bulk crystals, respectively.

method in high vacuum ($\sim 2\times 10^{-6}$ Torr). Commercially supplied powders of CuI with a purity of 99.9% were heated in a crucible, and the deposition rate, which was controlled by monitoring the frequency of a crystal oscillator, was about 0.1 nm/s. The deposition rate was calibrated by measuring the thickness of some thin films with a profilometer. The uncertainty of the layer thickness is estimated to be around 10%. After the deposition, no thermal treatment was performed. We note that the sticking coefficient of CuI to the sapphire substrate decreases above $\sim 200\,^{\circ}$C. The x-ray-diffraction patterns of the films were analyzed by the Cu $K\alpha$ line of a diffractometer. The $K\beta$ line was cut with a Ni filter. We performed absorption, luminescence, and reflection measurements. The absorption spectra were measured with a double-beam spectrometer. The excitation light of the luminescence spectra was a 325-nm line of a He-Cd laser, and the luminescence was analyzed with a 32-cm single monochromator. The probe light of the reflection spectra was produced by combination of a 100-W Xe lamp and a 32-cm single monochromator. The spectral resolution was 0.2 nm in all of the measurements. The sample temperature was controlled using a closed-cycle helium-gas cryostat.

III. RESULTS

Figure 1 shows the θ-2θ x-ray diffraction patterns measured at room temperature for CuI thin films with the thickness of 100 nm on the sapphire, quartz, and NaCl substrates. The radiation source is a Cu-$K\alpha$ line through a Ni filter. The 2θ angles of the (111) and (222) spacing of a CuI crystal with the zinc-blende structure are estimated to be 25.5° and 52.3°, respectively, from the lattice constant of a bulk crystal,[6] so that the diffraction patterns clearly indicate that the thin film grown on every substrate is preferentially oriented along the $\langle 111\rangle$ crystal axis. Similar patterns also have obtained in other CuI thin films. The accuracy and resolution of the diffractometer are not sufficient to discuss the strain of the films.

Figures 2 and 3 show absorption spectra measured at 10 K for the CuI thin films with the thickness of 10, 20, 50, and 100 nm grown on the sapphire and quartz substrates. The broken lines depicted at 3.06 and 3.70 eV represent the $Z_{1,2}$ and Z_3 exciton energies, respectively, in a CuI bulk crystal at 4.2 K.[6] The $Z_{1,2}$ exciton corresponds to the degenerate HH and LH excitons at the Γ point. As can be seen in the figures, the spectra include structures due to the $Z_{1,2}$ and Z_3 exciton

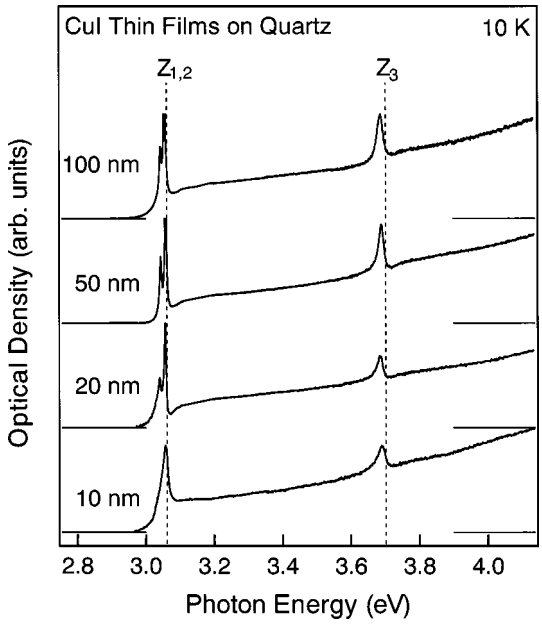

FIG. 3. Absorption spectra at 10 K for the CuI thin films with the thickness of 10, 20, 50, and 100 nm grown on the quartz substrate.

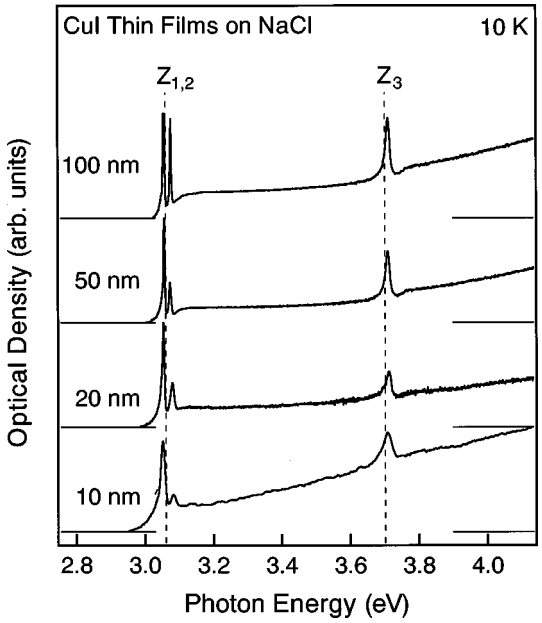

FIG. 4. Absorption spectra at 10 K for the CuI thin films with the thickness of 10, 20, 50, and 100 nm grown on the NaCl substrate.

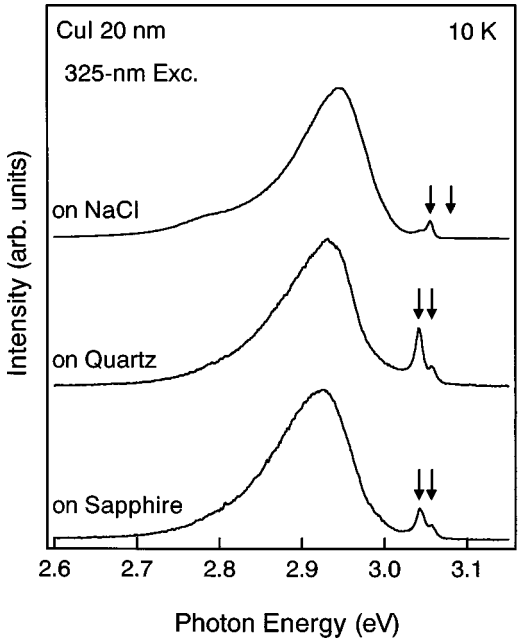

FIG. 5. Luminescence spectra with a 325-nm excitation at 10 K for the CuI thin films with the thickness of 20 nm grown on the sapphire, quartz, and NaCl substrates. The arrows represent the doublet-peak energies of the absorption spectra.

transitions, and the energies do not agree with those in the bulk crystal. It is noticed that all of the spectra except for those in the 10-nm films clearly show doublet structures around the $Z_{1,2}$ exciton peak: The stronger component has the higher energy. It is obvious from Figs. 2 and 3 that the splitting energies of the doublet structures do not depend on the film thickness up to 100 nm; 15 and 14 meV for the sapphire and quartz substrates, respectively. In the 10-nm films, the spectral-width broadening prevents observing the doublet structure of the $Z_{1,2}$ exciton.

Figure 4 shows absorption spectra measured at 10 K for the CuI thin films with the thickness of 10, 20, 50, and 100 nm grown on the NaCl substrate. The spectra include structures due to the $Z_{1,2}$ and Z_3 exciton transitions and show doublet structures around the $Z_{1,2}$ exciton energy. The splitting energies of the doublet structures are constant: 17 meV. These spectral profiles are similar to those in the sapphire and quartz substrates; however, the energy order of the stronger and weaker components of the doublet structure is reversed.

Figure 5 shows luminescence spectra at 10 K with the 325-nm excitation for the CuI thin films with the thickness of 20 nm grown on the sapphire, quartz, and NaCl substrates. The broad luminescence band in the low-energy region is considered to be due to the donor-acceptor-pair recombination which is observed in bulk crystals.[7] The arrows in the figure represent the doublet-peak energies of the absorption spectra. It is noticed that the luminescence spectra around the absorption edge consists of two bands. For the NaCl substrate, it is considered that the high-energy luminescence band originates from the free exciton because its peak energy just agrees with the low-energy absorption peak. The low-energy luminescence band appearing as a shoulder is considered to be due to a bound exciton:[8] The binding energy of the bound exciton, 12 meV, is equal to that in the bulk crystal. For the sapphire and quartz substrates, luminescence peak energies coincide with those of the absorption peaks. Then, we assign the luminescence bands to the free-exciton luminescence.

Next, we qualitatively discuss the doublet structure of the $Z_{1,2}$ exciton transition. The quantitative analysis will be described in the next section. The oscillator strength of the HH-exciton transition at the Γ point is considered to be three times stronger than that of the LH-exciton transition from the Bloch-function forms.[9] Thus, we assign the stronger component and the weaker one of the doublet structure to the HH- and LH-exciton transitions, respectively. There are two possible factors for causing the doublet structure: quantum size effects and strain effects. The fact that the splitting energy does not depend on the film thickness as shown in Figs. 2–4 indicates no possibility of the quantum size effect. Therefore, we focus only on the strain effect. It is well known that there are two types of the strain: lattice-mismatch and thermal strain, which are caused by the difference of the lattice constants and thermal expansion coefficients of the thin film and substrate. The possibility of the lattice-mismatch strain can be denied because of following reasons. The splitting due to the lattice-mismatch strain should depend on the film thickness because there exists a critical thickness for the elastic deformation. The lattice mismatch between CuI and NaCl is about 6.6%. Referring the results of the critical thickness as a function of the lattice mismatch in semiconductors,[10] the critical thickness of the CuI film on the NaCl substrate is estimated to be less than 1 nm. Nevertheless, as mentioned above, the magnitude of the splitting energy for the NaCl substrate does not depend on the film thickness up to 100 nm as shown in Fig. 4. In the case of the sapphire and quartz substrates, there is no meaning of the lattice mismatch because of the full difference of the crystal structure in sapphire and noncrystallinity in quartz. Consequently, it is considered

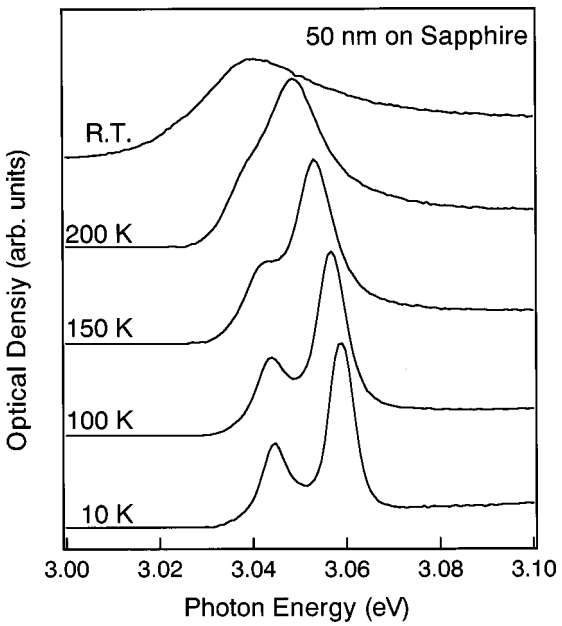

FIG. 6. Temperature dependence of the absorption spectra for the CuI thin films with the thickness of 50 nm grown on the sapphire substrate.

that the splitting of the HH- and LH-exciton energies is due to the thermal strain effect.

If the above consideration is true, the HH-LH splitting energy should depend on the measurement temperature. The temperature dependence of absorption spectra for the 50-nm thick CuI film grown on the sapphire substrate is shown in Fig. 6. Figure 7 shows the temperature dependence of the HH- (closed circles) and LH-exciton energies (open circles) of the CuI thin films with the thickness of 50 nm on (a) sapphire, (b) quartz, and (c) NaCl substrates. As can be seen in the figures, the splitting energies become smaller with the increase of the temperature. These results certainly indicate that the origin of the HH-LH splitting is the thermal strain effect.

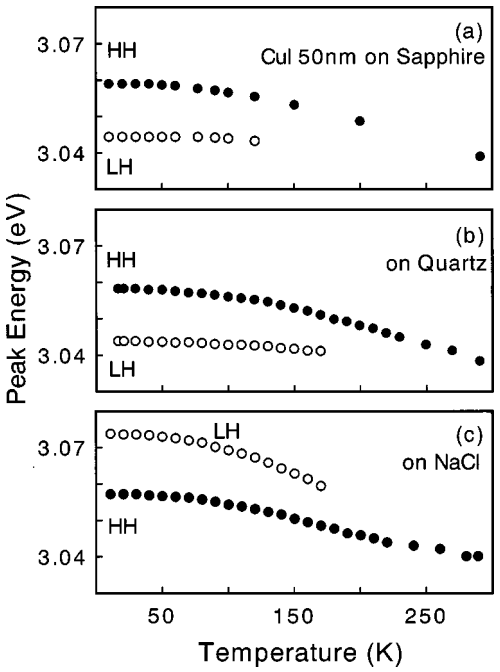

FIG. 7. Temperature dependence of the heavy-hole- (closed circles) and light-hole-exciton energies (open circles) of the CuI thin films with the thickness of 50 nm grown on (a) sapphire, (b) quartz, and (c) NaCl substrates.

IV. DISCUSSION

We quantitatively discuss the thermal strain effect on the HH- and LH-exciton energies of CuI thin films on the basis of a $k \cdot p$ perturbation theory.[11] The exciton-binding energy is hardly changed by the strain effect, so that we consider only the change of the Γ-conduction-band bottom and the Γ-valence-band top. Since the strain-induced-splitting energy in CuI films are much smaller than the spin-orbit-splitting energy ~ 630 meV as shown in Figs. 2–4, we can neglect the spin-orbit interaction in the $k \cdot p$ perturbation theory. The CuI thin films used in this study are preferentially oriented along the $\langle 111 \rangle$ crystal axis as shown in Fig. 1; therefore, we consider the deformation in the [111]-strained system. In this case, the strain-induced shifts of the heavy-hole and the light-hole energies at the Γ-valence-band top, ΔE_{hh} and ΔE_{lh}, are approximately given by[11]

$$\Delta E_{hh} = -\Delta E_H - \Delta E_S/2 \tag{1}$$

and

$$\Delta E_{lh} = -\Delta E_H + \Delta E_S/2, \tag{2}$$

where ΔE_H and ΔE_S, which are the hydrostatic and shear terms, are given by

$$\Delta E_H = 3a\{4C_{44}/(C_{11}+2C_{12}+4C_{44})\}\epsilon_{\parallel} \tag{3}$$

and

$$\Delta E_S = -2\sqrt{3}d\{(C_{11}+2C_{12})/(C_{11}+2C_{12}+4C_{44})\}\epsilon_{\parallel}. \tag{4}$$

Here, a and d represent the respective deformation potentials, C_{11}, C_{12}, and C_{44} are the elastic stiffness constants, and $\epsilon_{\parallel}$ is the in-plane strain. We define $\epsilon_{\parallel} > 0$ ($\epsilon_{\parallel} < 0$) for a tensile (compressive) strain. The s-like conduction-band state is affected only by the hydrostatic term of the strain:

$$\Delta E_c = 3c\{4C_{44}/(C_{11}+2C_{12}+4C_{44})\}\epsilon_{\parallel}, \tag{5}$$

where c is the deformation potential. Consequently, the energy shifts of the HH and LH excitons, ΔE_{HH} and ΔE_{LH}, are given by

$$\Delta E_{HH} = \Delta E_c - \Delta E_{hh} = \Delta E'_H + \Delta E_S/2 \tag{6}$$

and

$$\Delta E_{LH} = \Delta E_c - \Delta E_{lh} = \Delta E'_H - \Delta E_S/2, \tag{7}$$

where

$$\Delta E'_H = 3(a+c)\{4C_{44}/(C_{11}+2C_{12}+4C_{44})\}\epsilon_{\parallel}. \tag{8}$$

The magnitude of the thermal strain ϵ_t, which corresponds to $\epsilon_{\parallel}$, is given by

TABLE I. Values of deformation potentials, $a+c$ and d (Ref. 2), and stiffness constants, C_{11}, C_{12}, and C_{44} (Ref. 13) of CuI.

$a+c$ (eV)	d (eV)	C_{11} ($\times 10^{10}$ dyn/cm^2)	C_{12} ($\times 10^{10}$ dyn/cm^2)	C_{44} ($\times 10^{10}$ dyn/cm^2)
-1.1	-1.4	45.1	30.7	18.4

$$\epsilon_t = \int_{T_m}^{T_g} [\alpha_{CuI}(T) - \alpha_{sub}(T)]dT, \tag{9}$$

where T_g and T_m are the film-growth and measurement temperatures, respectively. The linear expansion coefficients of CuI and substrate materials are denoted by α_{CuI} and α_{sub}. The values of α essentially depend on temperature. The details of $\alpha_{sub}(T)$ for sapphire, quartz, and NaCl have been reported so far.[12,13] We obtained $\alpha_{CuI}(T)$ from the temperature dependence of the lattice constant.[6] We give an example of α at 293 K: 16×10^{-6}, 5×10^{-6}, 0.5×10^{-6}, and 39×10^{-6} deg^{-1} for CuI, sapphire, quartz, and NaCl, respectively. Since $\alpha_{CuI} > \alpha_{sub}$ ($\alpha_{CuI} < \alpha_{sub}$) for the sapphire and quartz substrates (NaCl substrate), the tensile (compressive) strain is applied to the CuI films. The thermal strain ϵ_t is calculated from Eq. (9): 4.7×10^{-3}, 5.9×10^{-3}, and -7.6×10^{-3} for the sapphire, quartz, and NaCl substrates, respectively, with $T_g = 443$ K and $T_m = 10$ K.

We first discuss the splitting energy, ΔE, of the HH and LH excitons. Since $\Delta E = \Delta E_{HH} - \Delta E_{LH}$ is equal to ΔE_S from Eqs. (6) and (7), the theoretical value of ΔE is calculated from Eq. (4): 14, 17, and -22 meV for the sapphire, quartz, and NaCl substrates, respectively. The calculation parameters for the strain effect are listed in Table I. Table II shows the calculated values of ϵ_t and ΔE_{cal}, and experimental values, ΔE_{exp}, obtained from the absorption spectra (10 K) of the 50-nm films, in which the widths of the absorption bands are the narrowest as shown in Figs. 2–4. The minus sign for ΔE_{cal} and ΔE_{exp} means that the LH exciton has higher energy than the HH exciton. It is obvious that the calculated results well explain the substrate-material dependence of the order of the HH- and LH-exciton energies. Thus, we conclude that the observed doublet structure of the $Z_{1,2}$-exciton absorption originates from the thermal-strain-induced splitting of the HH- and LH-exciton energies.

Next, we discuss the center energy, E_0, of the splitting HH and LH excitons. From Eqs. (6) and (7), the energy shift of E_0 is determined by the hydrostatic term $\Delta E'_H$. Since $a+c<0$, it is expected that the tensile (compressive) strains induce the low-energy (high-energy) shift of E_0: E_0 is shifted to the low-energy (high-energy) side for the sapphire and quartz substrates (NaCl substrate). The calculated values of $\Delta E'_H$ are -6, -8, and 10 meV for the sapphire, quartz, and NaCl substrates, respectively. These agree with the experimental results obtained from the absorption spectra of the 50-nm films shown in Figs. 2–4: -4, -5, and 10 meV for the sapphire, quartz, and NaCl substrates, respectively.

Finally, we discuss the film-thickness dependence of the thermal strain in the CuI films. As shown in Figs. 2, 3, and 4, the exciton energies are constant in the thickness region thinner than 100 nm: This indicates that the thermal strain is unchanged. The absorption spectra for thick films could not be measured because of saturation of the absorption intensity. So we measured reflection spectra for the films thicker than 100 nm. Figure 8 shows reflection spectra at 10 K for the CuI films with the thickness of 100, 300, 400, 500, 1000, and 3000 nm grown on the sapphire substrate. The broken and dotted lines represent the HH- and LH-exciton energies in the 50-nm thick film, respectively. We consider the peak energies of the reflection spectra to be exciton energies since the absorption-peak energies in the 50-nm film agree with reflection-peak energies in the 100-nm film. The stronger component and the weaker one in the reflection spectra correspond to the HH- and LH-exciton transitions, respectively. The arrows indicate the peak energies of the LH-exciton reflection. Structures due to the Fabry-Perot interference are remarkably superimposed in the low-energy side of the LH-exciton band for the films thicker than 100 nm. The splitting

TABLE II. Values of thermal strains (ϵ_t), splitting energies of the heavy-hole and light-hole excitons obtained from the calculation (ΔE_{cal}) and the absorption spectra (ΔE_{exp}) for CuI thin films with the thickness of 50 nm.

Substrates	ϵ_t	ΔE_{cal} (meV)	ΔE_{exp} (meV)
Al_2O_3	4.7×10^{-3}	14	15
quartz	5.9×10^{-3}	17	14
NaCl	-7.6×10^{-3}	-22	-17

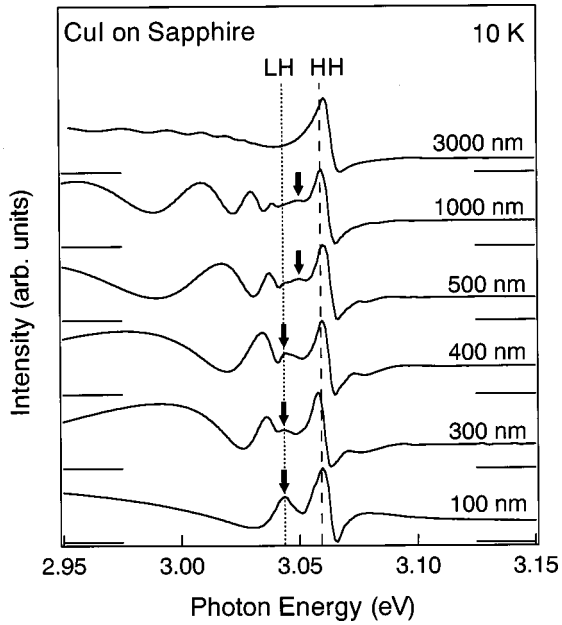

FIG. 8. Reflection spectra at 10 K for the CuI thin films with the thickness of 100, 300, 400, 500, 1000, and 3000 nm grown on the sapphire substrate. The broken and dotted lines represent the heavy-hole- and light-hole-exciton energies in the 50-nm film, respectively. The arrows indicate the peak energies of the light-hole-exciton reflection.

of the HH and LH excitons begins to become small at 500 nm and disappears at 3000 nm. This result indicates that the thermal strain begins to relax at 500 nm and fully vanishes at the 3000-nm thickness. As can be seen in the figure, the transition energy of the HH exciton almost does not change in contrast with that of the LH exciton. From Eqs. (4)–(8), the following relations of the exciton-energy shift and the in-plane strain are obtained: $\Delta E_{HH} \simeq 0.08\ \epsilon_{\parallel}$ and $\Delta E_{LH} \simeq -2.8\ \epsilon_{\parallel}$. As a result, the HH-exciton energy is much less insensitive to the variance of the strain than the LH-exciton energy.

V. CONCLUSION

We have investigated the thermal strain effect on the exciton in CuI thin films with a thickness of 10–3000 nm. The thin films were grown by vacuum evaporation onto (0001) Al_2O_3, fused silica (quartz), and (001) NaCl substrates. We have investigated x-ray-diffraction patterns and optical absorption, luminescence, and reflection spectra of the films. From the x-ray-diffraction patterns, we confirmed that the crystalline thin films preferentially oriented along the $\langle 111 \rangle$ crystal axis for all the substrates. The doublet structures around the $Z_{1,2}$ exciton energy were observed in the absorption spectra for all of the thin films in the 10–1000 nm range. We have assigned the stronger component and the weaker one of the doublet structure to the HH- and LH-exciton transitions, respectively. The magnitude of the splitting energy does not depend on the film thickness in the 100–1000 nm range and becomes small with the increase of the measurement temperature. From the results, we conclude that the doublet structures are due to the splitting of the HH- and LH-exciton energies, which are caused by the biaxial strains arising from the difference of the thermal expansion coefficients of CuI and the substrate, the so-called thermal strain effect. The HH exciton has a higher energy than the LH exciton for the sapphire and quartz substrates, while the energy order of the HH and LH excitons is reversed for the NaCl substrate. Since the thermal expansion coefficient of CuI is larger (smaller) than those of the sapphire and quartz (NaCl) substrate, the tensile (compressive) strain is applied to the films. The change of the direction of the thermal strain results in the reverse of the energy order of the HH and LH excitons. The shifts and the energy order of the exciton energies due to the thermal strain effect are successfully analyzed on the basis of a $k \cdot p$ perturbation theory. We also have investigated the film-thickness dependence of the thermal strain effect by measuring the reflection spectra for the films thicker than 100 nm. The critical thickness for the thermal strain relaxation is estimated to be about 400 nm.

[1] For a review of excitonic properties of cuprous halides, see M. Ueta, H. Kanzaki, K. Kobayashi, Y. Toyozawa, and E. Hanamura, *Excitonic Processes in Solids* (Springer-Verlag, Berlin, 1986).

[2] A. Blacha, S. Ves, and M. Cardona, Phys. Rev. B **27**, 6346 (1983).

[3] L. A. Ageev, V. K. Miloslavskii, and T. I. Maksimenko, Fiz. Tverd. Tela **16**, 2894 (1974) [Sov. Phys. Solid State **16**, 1873 (1975)].

[4] Z. K. Tang, A. Yanase, T. Yasui, Y. Segawa, and K. Cho, Phys. Rev. Lett. **71**, 1431 (1993).

[5] M. Nakayama, A. Soumura, K. Hamasaki, T. Takeuchi, and H. Nishimura, Phys. Rev. B **55**, 10 099 (1997).

[6] *Physics of II-VI and I-VII Compounds, Semimagnetic Semiconductors*, edited by O. Madelung, Landolt-Börnstein, New Series, Group 3, Vol. 17, Part b (Springer, Berlin, 1982), pp. 270, 271, and 501.

[7] V. A. Nikitenko and S. G. Stoyukhin, Opt. Spektrosk. **54**, 193 (1983) [Opt. Spectrosc. **54**, 111 (1983)].

[8] T. Goto, T. Takahashi, and M. Ueta, J. Phys. Soc. Jpn. **24**, 314 (1968).

[9] E. O. Kane, J. Phys. Chem. Solids **1**, 249 (1957).

[10] I. J. Fritz, Appl. Phys. Lett. **51**, 1080 (1987).

[11] M. Chandrasekhar and F. H. Pollak, Phys. Rev. B **15**, 2127 (1977).

[12] *American Institute of Physics Handbook*, 3rd ed. (McGraw-Hill Book Company, New York, 1972), pp. 4-136 and 4-139.

[13] R. C. Hanson, J. R. Hallberg, and C. Schwab, Appl. Phys. Lett. **21**, 490 (1972).